



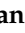

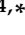


## Article

# Mapping Archaeal Diversity in Soda Lakes by Coupling 16S rRNA PCR-DGGE Analysis with Remote Sensing and GIS Technology

Naglaa Elshafey<sup>1</sup>, Samy Selim<sup>2,\*</sup> , Asmaa H. Mohammed<sup>3</sup>, Nashwa Hagagy<sup>4,5</sup> , Mennatalla Samy<sup>6</sup>, Ehab M. Mostafa<sup>7</sup> , Fatmah A. Safhi<sup>8</sup> , Salha M. Alshamrani<sup>9</sup> , Amna Saddiq<sup>4</sup>, Salam S. Alsharari<sup>10</sup>, Dalia G. Aseel<sup>11</sup>, Iram Hafiz<sup>12</sup>, Amr Elkelish<sup>5</sup>  and Leonardo M. Pérez<sup>13,14,\*</sup> 

- <sup>1</sup> Botany and Microbiology Department, Faculty of Science, Al-Arish University, Al-Arish 45511, Egypt; n\_fathi@aru.edu.eg
- <sup>2</sup> Department of Clinical Laboratory Sciences, College of Applied Medical Sciences, Jouf University, Sakaka 72341, Saudi Arabia
- <sup>3</sup> Marine Sciences Department, National Authority for Remote Sensing and Space Sciences, Cairo P.O. Box 1564, Egypt; asmahassan@narss.sci.eg
- <sup>4</sup> Department of Biology, College of Science & Arts at Khulis, University of Jeddah, Jeddah 21959, Saudi Arabia; niibrahem@uj.edu.sa (N.H.); aansaddiq@uj.edu.sa (A.S.)
- <sup>5</sup> Botany and Microbiology Department, Faculty of Science, Suez Canal University, Ismailia 41522, Egypt; amr.elkelish@science.suez.edu.eg
- <sup>6</sup> Department of Communications and Computers Engineering, The Higher Institute of Engineering, El-Shorouk City 11837, Egypt; mentalla.samy@sha.edu.eg
- <sup>7</sup> Department of Pharmacognosy, College of Pharmacy, Jouf University, Sakaka 72341, Saudi Arabia; emmoustafa@ju.edu.sa
- <sup>8</sup> Department of Biology, College of Science, Princess Nourah bint Abdulrahman University, P.O. Box 84428, Riyadh 11671, Saudi Arabia; faalsafhi@pnu.edu.sa
- <sup>9</sup> Department of Biology, College of Science, University of Jeddah, Jeddah 21577, Saudi Arabia; smalshmrane@uj.edu.sa
- <sup>10</sup> Biology Department, College of Science, Jouf University, Sakaka P.O. Box 72341, Saudi Arabia; ssshrary@ju.edu.sa
- <sup>11</sup> Plant Protection and Biomolecular Diagnosis Department, Arid Lands Cultivation Research Institute (ALCRI), City of Scientific Research and Technological Applications (SRTA, City), New Borg El-Arab City 21934, Egypt; daseel@srtacity.sci.eg
- <sup>12</sup> Institute of Chemistry, University of Sargodha, Sargodha 40100, Pakistan; iram.hafiz@uos.edu.pk
- <sup>13</sup> Facultad de Química e Ingeniería del Rosario, Pontificia Universidad Católica Argentina (UCA), Av. Pellegrini 3314, Rosario S2002QEO, Argentina
- <sup>14</sup> National Scientific and Technical Research Council (CONICET), Ministry of Science, Technology and Productive Innovation, Godoy Cruz 2290, Buenos Aires C1425FQB, Argentina
- \* Correspondence: sabdulsalam@ju.edu.sa (S.S.); leonardoperez@uca.edu.ar or perez@inv.rosario-conicet.gov.ar (L.M.P.)
- † Current Address: Laboratory of Sanitary and Environmental Microbiology (MSMLab), Polytechnic University of Catalonia (UPC-BarcelonaTech), Rambla de Sant Nebridi 22, 08222 Terrassa, Barcelona, Spain.



**Citation:** Elshafey, N.; Selim, S.; Mohammed, A.H.; Hagagy, N.; Samy, M.; Mostafa, E.M.; Safhi, F.A.; Alshamrani, S.M.; Saddiq, A.; Alsharari, S.S.; et al. Mapping Archaeal Diversity in Soda Lakes by Coupling 16S rRNA PCR-DGGE Analysis with Remote Sensing and GIS Technology. *Fermentation* **2022**, *8*, 365. <https://doi.org/10.3390/fermentation8080365>

Academic Editor: Mădălin-Iancu Enache

Received: 15 June 2022

Accepted: 25 July 2022

Published: 30 July 2022

**Publisher's Note:** MDPI stays neutral with regard to jurisdictional claims in published maps and institutional affiliations.



**Copyright:** © 2022 by the authors. Licensee MDPI, Basel, Switzerland. This article is an open access article distributed under the terms and conditions of the Creative Commons Attribution (CC BY) license (<https://creativecommons.org/licenses/by/4.0/>).

**Abstract:** The haloarchaeal diversity of four hypersaline alkaline lakes from the Wadi El-Natrun depression (Northern Egypt) was investigated using culture-independent polymerase chain reaction-denaturing gradient gel electrophoresis (PCR-DGGE) of 16S rRNA gene phylotypes, which was combined with remote sensing and geographic information system (GIS) data to highlight the distribution pattern of the microbial diversity in water and sediment samples. The majority of archaeal sequences identified in all four lakes belonged to the phyla Euryarchaeota and Crenarchaeota. Sediment samples from Beida Lake and water samples from El-Hamra Lake showed the highest levels of archaeal diversity. Sequence similarities  $\geq 95\%$  were found between six of the acquired clones and uncultured *Halorhabdus*, Euryarchaeota, and archaeon clones. In addition, two clones shared a high level of sequence similarity (97%) with unclassified archaea, while other nine clones exhibited 96% to 99% sequence similarity with uncultured archaeon clones, and only one clone showed 97% identity with an uncultured Crenarchaeota. Likewise, 7 DGGE bands presented a sequence similarity of 90 to 98% to *Halogranum* sp., *Halalkalicoccus tibetensis*, *Halalkalicoccus jeotgali*, uncultured *Halorubrum*,

*Halobacteriaceae* sp., or uncultured haloarchaeon. In conclusion, while the variety of alkaliphilic haloarchaea in the examined soda lakes was restricted, the possibility of uncovering novel species for biotechnological applications from these extreme habitats remains promising.

**Keywords:** haloalkaliphilic archaea; soda lakes; DGGE; GIS-integrated remote sensing data; microbial diversity mapping

## 1. Introduction

Soda lakes are saline and alkaline water storage reserve basins that have developed as a result of geological activity. These ecosystems are considered to have existed since the first geological records of the world. In fact, soda lakes occur all over the world, with the best-known examples found along the East African rift and western USA [1–3]. Among them, the Wadi El-Natrun is an endorheic depression in the Sahara Desert of northern Egypt that contains several alkaline lakes, natron-rich salt deposits, salt marshes, and freshwater marshes. Historically, this valley was part of an old branch of the Nile River that deteriorated with time [2]. The groundwater of the Pliocene aquifer in Wadi El-Natrun represents the primary source of reliable water for drinking and agriculture. However, its quality has been affected by the presence of inland saline water preserved during the Miocene [3]. In addition, in recent years, there has been an increase in cultivated areas in the zone that have impacted the properties of the aquifers due to rising water discharges [1]. However, the valley is still considered a unique aquatic ecosystem, especially for the presence of hypersaline and alkaline lakes rich in minerals such as sulphate ( $\text{SO}_4^{2-}$ ), chloride ( $\text{Cl}^-$ ), carbonate ( $\text{CO}_3^{2-}$ ), sodium ( $\text{Na}^+$ ), and magnesium ( $\text{Mg}^{2+}$ ). Moreover, the color of these lakes is reddish blue because their water is saturated with natron salt [2,3].

Many studies regarding the geology, hydrogeology, and mineralogy of saline deposits from Wadi El-Natrun were performed using hyperspectral remote sensing technology to map the mineral content of these areas [4,5]. Accordingly, the lakes located in the Wadi El-Natrun depression are thalassic saline aquatic environments characterized by the presence of  $\text{Na}^+$  and hydrogen carbonate ( $\text{HCO}_3^-$ ) as the major ions. Although the salinity of the soda lakes from Wadi El-Natrun is lower than that of other saline lakes, the pH of these environments is moderately alkaline ( $\text{pH} \approx 8-9$ ) [1–3].

Many saline soda lakes are highly productive and contain different microbial populations despite being extreme environments [6]. The microbial communities associated with soda lakes have been investigated in several hypersaline ecosystems, including the Altai region (Russia) [7,8], Rift Valley (Kenya) [9], Mono Lake (California, USA) [10], and Searles Lake (California, USA) [11]. However, to date there is still limited information about the microbial diversity of such attracting environments. Compared to other marine and aquatic habitats, the microbial diversity found in the alkaline lakes of Wadi El-Natrun is limited and mostly dominated by the bacterial phyla Firmicutes, Bacteroidetes, and Proteobacteria (distributed in the classes Alpha and Gamma), and two orders of Archaea (Halobacteriales and Methanosarcinales) [12]. Several alkaliphilic Halobacteria belonging to the genera *Natronobacterium*, *Natronococcus*, *Natronomonas*, *Natronolimnobi*, *Natronorubrum*, *Natrialba*, *Natrinema*, *Natronoarchaeum*, *Halalkalicoccus* which, *Halorubrum*, and *Haloterrigena* also have been described in these hypersaline environments, including the extremely saline and alkaline lakes of Wadi El-Natrun [13–15]. In addition, novel haloarchaea classified as *Halodesulfurarchaeum formicicum* sp. nov., *Salinarchaeum chitinilyticum* sp. nov., *Halomarina rubra* sp. nov., and *Halococcoides cellulovorans* sp. nov. were recently isolated and classified from different saline habitats [15–18]. These groups of bacteria are very interesting from an environmental perspective since microorganisms belonging to the haloarchaea group possess many unusual features.

Regarding this, *Haloarchaea*, the extremely halophilic branch of the *Archaea* domain, is a physiologically and morphologically unique group with chemoorganotrophic-aerobic

metabolism. Members of this class require high salt concentrations to grow, with most species requiring more than 1.5 M NaCl to survival and to preserve the integrity of their cells [19–24]. Most *Haloarchaea* species, including *Halobacterium*, *Halorubrum*, *Haloarcula*, *Haloferax*, *Halococcus*, *Halobaculum*, and *Natrialba* spp., grow best at neutral pH [25–27]. Moreover, alkaliphilic halobacteria, such as *Natronomonas* and *Natronobacterium* spp., grow in alkaline-saline environments and require  $\text{pH} \geq 8.5$  to properly develop [21,28]. At least 51 genera have been characterized among the Halobacteriales showing considerable eco-physiological diversity [29]. These extremophilic microorganisms are already used for multiple biotechnological applications such as the production of bacteriorhodopsin,  $\beta$ -carotene, polyhydroxyalcanoates, polysaccharides, and enzymes, as well as for use in oil recovery, drug screening, and the biodegradation of toxic compounds [30–32]. Therefore, Haloarchaea are very attractive organisms for biologists due to their extremophilic nature, anaerobic lifestyle, salinity, and toxic metals tolerance, as well as for their resistance to high levels of ultraviolet and ionizing radiation [19–31].

Over the last few years, research has focused on the study of prokaryotic diversity and community structure in several saline ecosystems from different geographical areas using techniques such as denaturing gradient gel electrophoresis (DGGE), single-strand-conformation polymorphism (SSCP), PhyloChip, and 16S rRNA gene amplicon sequencing libraries [33–40]. These techniques have proven to be successful in evaluating microbial diversity and identifying new bacterial and archaeal species in complex environmental niches [24–28,33–40]. The first ecological study on the microbial communities of three soda lakes located in the Wadi El-Natron depression based on the analysis of 16S rRNA sequences was achieved by [12,41]. Likewise, DGGE is a low-cost fingerprinting technology that also can be used to analyze complex communities, reveal population shifts, and detect sequence heterogeneities. While bands can be cut off, re-amplified and sequenced, it is possible to obtain taxonomic information using DGGE profiling [38–40].

In this study, we assessed the archaeal diversity in four hypersaline alkaline lakes of Wadi El-Natron by PCR-DGGE and 16S rRNA gene sequence analysis. In addition, distinct chemical zones (i.e., water and sediment) as well as the microbial diversity of these extreme habitats were mapped using hyperspectral remote sensing data and GIS.

## 2. Materials and Methods

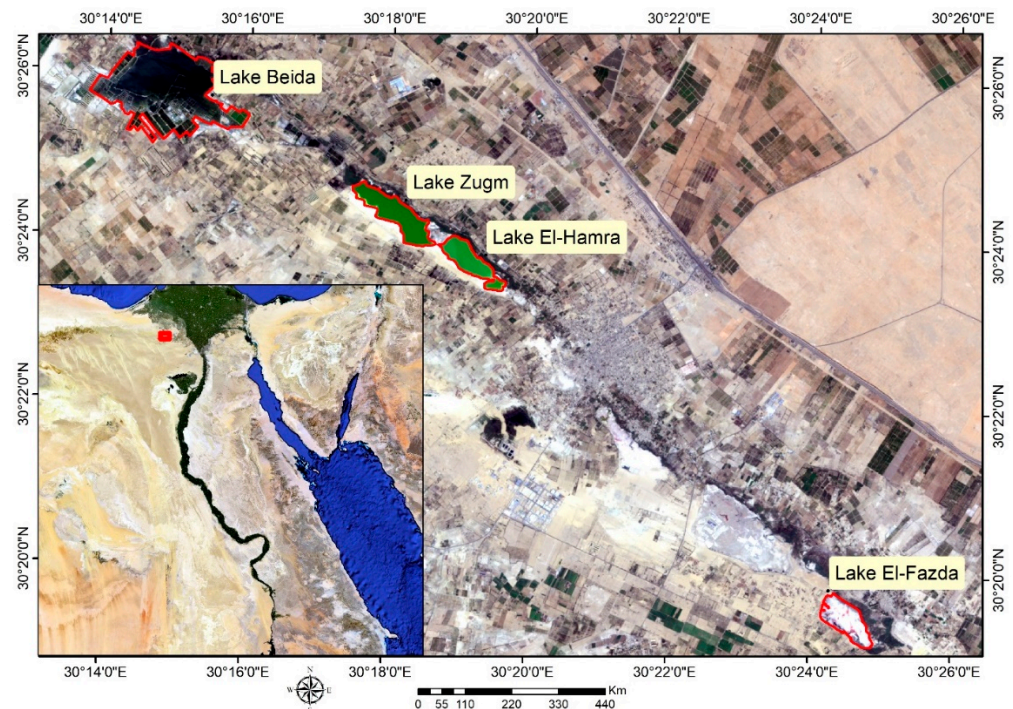
### 2.1. Site Description and Sample Collection

Water and sediment samples (including salt crystals) were collected from four soda lakes located in the Wadi El-Natron depression in the Libyan Desert (Northern Egypt) corresponding to El-Hamra Lake (30°23′48.28″ N, 30°19′13.39″ E), Zugm Lake (30°23.917′ N, 30°18.383′ E), Beida Lake (30°25′57″ N, 30°14′30″ E), and El-Fazda Lake (30°19′43.50″ N, 30°24′29.68″ E) (Figure 1). The samples were collected into sterile glass flasks and stored at 4 °C until arrival to the lab for further analysis. The electrical conductivity (EC) and pH of the water samples were measured using calibrated electrodes (Hanna Instruments Inc., Smithfield, RI, USA). The contents of  $\text{Ca}^{2+}$ ,  $\text{Mg}^{2+}$ ,  $\text{Na}^{+}$  and  $\text{K}^{+}$  were respectively quantified by flame atomic absorption using a Perkin Elmer 2380 spectrophotometer (Perkin Elmer Inc., Woodbridge, ON, Canada). The total amount of  $\text{Cl}^{-}$  and the  $\text{HCO}_3^{-}/\text{CO}_3^{2-}$  ratio were estimated by traditional argentometric and acid–base titration methods, respectively. The  $\text{SO}_4^{2-}$  concentration was estimated using the turbidimetric method, as described by [42].

### 2.2. Molecular Assays

#### 2.2.1. DNA Extraction

Genomic DNA was extracted from 100 mL of filtered water samples (through 0.2  $\mu\text{m}$  membrane filters) and 1.0 g of sediment or salt crystal samples by using the UltraClean soil DNA extraction kit (catalog no.12900-10, MoBio Laboratories, Inc., Carlsbad, CA, USA), following the manufacturer’s instructions. The isolated genomic DNA was then used as a template for qPCR analyses.



**Figure 1.** Location map of soda lakes from Wadi El-Natron depression analyzed in the present study.

### 2.2.2. Quantitative PCR (*qPCR*)

Archaeal 16S rRNA gene levels in the isolated environmental DNA were quantified by *qPCR* using a CFX96 Touch Real-Time PCR detection system (Bio-Rad, Segrate, MI, Italy). For each sample, reactions were achieved in triplicate ( $n = 3$ ) within optical tubes in a final volume of 20  $\mu\text{L}$  containing 2  $\mu\text{L}$  DNA template, 10  $\mu\text{L}$  SYBR Green TM*qPCR* Master Mix (Bio-Rad, Segrate, MI, Italy), 7.4  $\mu\text{L}$  DNase-free water, and 0.3  $\mu\text{L}$  of each primer [40,43]. For quantification of archaeal 16S rRNA gene copies, the specific primers used for DNA amplification were 0344F (5'-ACGGGGCGCAGCAGGCGCGA-3') and 0025R (5'-GGACTACVSGGTATCTAAT-3') per reaction.

The cycling settings were as follows: initial denaturation at 95 °C for 30 s, followed by 35 cycles of denaturation (at 95 °C for 5 s), annealing (at 60 °C for 20 s), and extension (at 72 °C for 20 s). A melting curve was generated at the end of each assay to verify the specificity of amplicons. Archaeal 16S rRNA gene copy number was reported per gram dry weight of sediment/salt crystal or mL of water sample, respectively. The PCR protocol was optimized and verified according to [44].

### 2.2.3. DGGE Analysis

For DGGE analysis, total archaeal 16S rRNA genes obtained from the environmental samples were further amplified using nested PCR. All sets of primers used in this study are summarized in Table 1. The reaction conditions were as formerly described [45–49]. For the first step, the PCR mixture contained 1.5  $\mu\text{L}$   $\text{MgCl}_2$  (1.5 mM), 1  $\mu\text{L}$  bovine serum albumin (BSA, 10  $\mu\text{g}$ ), 0.5  $\mu\text{L}$  dNTP (200  $\mu\text{M}$  each dNTP), 0.5  $\mu\text{L}$  of primers A2F and 1492R (200 nM), 0.25  $\mu\text{L}$  Taq DNA polymerase (1.5 U), 2.5  $\mu\text{L}$  DNA template, and 16.25  $\mu\text{L}$  sterile nanopure water in 2.5  $\mu\text{L}$  PCR buffer (1  $\times$ ). PCR amplifications were completed in a DNA Engine Dyad Thermal cycler gradient block (MJ Research, Quebec, Canada) using the following program: 30 reaction cycles, pre-denaturation (95 °C, 5 min), denaturation (94 °C, 1 min), annealing (34.5 °C, 1 min), extension (72 °C, 1 min), and a final extension at 72 °C for 10 min. For the nested PCR second round, an identical reaction mixture as described above was prepared, but using primers SAF-GC and PARCH519R [48]. The amplified DNA was stored at  $-20$  °C.

**Table 1.** PCR primers used in this study.

Primer Pair	Sequence (5′–3′) <sup>a</sup>	Target of 16S rRNA Gene	Binding Position <sup>b</sup>	Reference
1492R A2F	GGTTACCTTGTTACGACT T TTCCGGTTGATCCYGCCGGA		1492–1510	[50]
SAF-GC <sup>c,d</sup> PARCH519R	SA1f-CCTAYGGGGCGCAGCAGG SA2f-CCTACGGGGCGCAGAGGG TTA CCG CGG CKG CTG		341–358	[51] [52]
M13R-GC	SAaf-CAGGAAACAGCTATGACG GGCGGGGCGGGGGCACGGGG GGCCTACGGGGCGCAGCAGG SAbf-CAGGAAACAGCTATGACG GGGGCGGGGCGGGGGCACGG GGCCTATGGGGCGCAGCAGG	<i>Archaea 16S rRNA</i>	519–533	[48]
M13F <sup>e</sup>	GTA AACGACGGCCAG			

<sup>a</sup> D = G, A or T; H = A, T or C; K = G or T; M = A or C; R = A or G; S = G or C; W = A or T; Y = C or T. <sup>b</sup> Based on *Escherichia coli* numbering except for the *mcrA*, which corresponds to *Methanothermobacter marburgensis* (CP001710), and *dsrAB* and *dsrB* gene, which correspond with *Desulfovibrio vulgaris* (CP002297) numbering. <sup>c</sup> For DGGE, this primer has the GC-clamp at the 5′ end, CGCCCGCCGCGCGCGGGCGGGGCGGGGCGGGGGCACGGGGGG. <sup>d</sup> Primer SaF-GC is a mixture of primers Sa1F and Sa2F at a molecular ratio of 2:1. <sup>e</sup> There are multiple versions of the M13 primers, and sequencing should be carried out with the versions described here.

The DGGE was run in a DCode™ Universal Mutation detection system (Bio-Rad Laboratories, Segrate MI, Italy) catalog number 170-9080 as described by [46]. Briefly, a 6% polyacrylamide gel with a gradient of 30–80% denaturant agent was cast by mixing solutions of 30% in 80% denaturant agent (100% denaturant agent was a mixture of 7 M urea and 40% deionized formamide). Five hundred ng of PCR product were loaded for each sample, and the gels were run at 100 V for 18 h at 60 °C in 1 × TAE buffer (40 mM Tris-HCl pH 7.4, 20 mM sodium acetate, 1 mM EDTA). Then, the gel was stained with SYBR Gold (Invitrogen) for 30 min and observed under UV light. Gel pictures were taken with a Gene Genius Bio Imaging System (Syngene). Prominent bands were excised from the gels, suspended in milli-Q water overnight, and re-amplified by PCR using the archaeal primers SAf-GC-M13R and PARCH519R according to [48]. Finally, the re-amplified PCR products were sequenced at MacroGen (<http://www.dna.macrogen.com> accessed on 20 February 2022). The sequencing data were analyzed using the Chromas Lite software package version 2.1.1. (<http://www.technelysium.com.au/> accessed on 20 February 2022). A nucleotide BLAST search (<http://www.ncbi.nlm.nih.gov/BLAST/> accessed on 20 February 2022) was carried out to obtain evidence on the phylogenetically closest relatives. The sequences were aligned by ClustalW and used to build the phylogenetic tree [49]. Alignments were edited using BioEdit Sequence Alignment Editor version 7.0.9.0, and regions of ambiguous alignment were removed. Pairwise similarities of 16S rRNA sequences were estimated using the MEGA 6.0 phylogeny software.

### 2.3. Remote Sensing

#### 2.3.1. Image Acquisition

One scene located on path 177 and row 39 of the Landsat-5 Thematic Mapper (TM) was used to derive the different maps obtained in the present study. The data were acquired in October 2010. The image consisted of seven spectral bands with a spatial resolution of 30 m for multispectral bands from 1 to 5, and 7 (visible, near-infrared, and two bands of shortwave).

#### 2.3.2. Image Processing

The pre-processing of the satellite scene was performed in two steps for the atmospheric correction of the multispectral image by removing noise influence. The first step of radiometric calibration was assessed by converting each pixel intensity value of the image (represented by a digital number) to a physical value of reflectance. In the second step,

the quantized pixel values were converted to surface reflectance data using the FLAASH correction tool in the ENVI software package (version 5.3). Then, the surface reflectance data were processed using the normalized difference water index (NDWI) to delineate open water features and separate surface water from land (moisture soil and salts) according to the following equation [53]:

$$NDWI = (Green - NIR)/(Green + NIR) \tag{1}$$

A threshold NDWI value of 30% was used to create the surface water map of the study area.

### 2.4. Statistical Analysis

Data were analyzed using Minitab 19 and visualized using GraphPad 8. A *p* value of 0.05 was considered significant. Tukey test for pairwise and one-way ANOVA comparisons was used for *post hoc* analysis of all group interactions. *Post hoc* analysis results are shown as letters, with groups that share the same letter being non-significantly different, and distinct letters expressing significant differences across various groups.

## 3. Results and Discussion

### 3.1. Physicochemical Analysis

Wadi EL-Natron is one of the most prominent geographical features in the northern Western Desert of Egypt. Both the saline lakes located in Wadi El-Natron and the ones in Florida (USA) are the only two worldwide cases of soda lakes used for natural salt production [54]. A few types of organisms can live in saltern crystallizer ponds, including rare eukaryotes and some halophilic prokaryotes [55]. The physicochemical analyses performed on water and sediment samples collected from the studied lakes showed that these alkaline hypersaline habitats are suitable for the development of haloalkaliphilic archaea, as reported by [56,57]. As shown in Table 2, the average pH values for all samples tested ranged from  $8.56 \pm 0.41$  to  $9.03 \pm 0.38$ . This relatively high alkalinity is associated with an elevated content of  $CO_3^{2-}$  and  $HCO_3^-$  (Table 2). In addition, the average concentrations of  $Ca^{2+}$  and  $Mg^{2+}$  were comparatively low. According to the classification proposed by [58], all of the studied lakes can be classified as brines due to the predominance of  $Cl^-$  over  $SO_4^{2-}$  and the ratio of  $Ca^{2+}$  to  $Na^+$  (Table 2). Brines are important sources of common salt (NaCl),  $Ca^{2+}$ ,  $Mg^{2+}$ ,  $K^+$ , and other materials, making them very attractive for mineral extraction. Alternatively, a visual examination of sediment samples taken from the investigated soda lakes revealed the existence of thin pink layers of purple photosynthetic bacteria and red halophilic archaea, as well as dense black layers of decomposed organic debris and sulfide minerals. The same outcomes were previously detailed by [12].

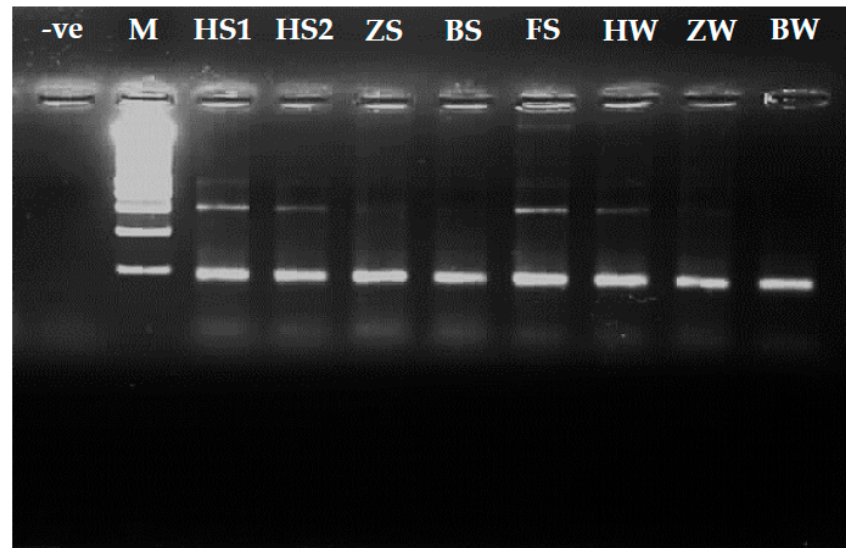
**Table 2.** Physicochemical analysis of water and sediment samples collected from soda lakes of Wadi El-Natron.

Sample ID	pH	EC (dSm <sup>-1</sup> )	Na <sup>+</sup>	K <sup>+</sup>	Ca <sup>2+</sup>	Mg <sup>2+</sup>	CO <sub>3</sub> <sup>2-</sup>	HCO <sub>3</sub> <sup>-</sup>	Cl <sup>-</sup>	SO <sub>4</sub> <sup>2-</sup>
H	9.03 ± 0.38 <sup>a</sup>	151.3 ± 2.5 <sup>c</sup>	24.24 ± 1.14 <sup>b</sup>	0.110 ± 0.010 <sup>a</sup>	0.10 ± 0.01 <sup>c</sup>	0.48 ± 0.04 <sup>c</sup>	10.80 ± 0.54 <sup>b</sup>	7.75 ± 0.28 <sup>b</sup>	26.18 ± 1.20 <sup>bc</sup>	6.00 ± 0.24 <sup>b</sup>
Z	8.89 ± 0.44 <sup>a</sup>	188.3 ± 3.8 <sup>b</sup>	31.42 ± 1.11 <sup>a</sup>	0.057 ± 0.003 <sup>c</sup>	0.23 ± 0.01 <sup>b</sup>	0.72 ± 0.05 <sup>a</sup>	21.30 ± 0.11 <sup>a</sup>	13.95 ± 1.10 <sup>a</sup>	28.95 ± 1.20 <sup>b</sup>	5.48 ± 0.35 <sup>bc</sup>
B	8.70 ± 0.31 <sup>a</sup>	137.4 ± 2.7 <sup>d</sup>	21.96 ± 1.20 <sup>b</sup>	0.076 ± 0.005 <sup>b</sup>	0.32 ± 0.01 <sup>a</sup>	0.42 ± 0.03 <sup>c</sup>	9.33 ± 0.46 <sup>c</sup>	6.60 ± 0.24 <sup>bc</sup>	24.65 ± 1.10 <sup>c</sup>	5.04 ± 0.25 <sup>c</sup>
F*	N.D.	N.D.	N.D.	N.D.	N.D.	N.D.	N.D.	N.D.	N.D.	N.D.
HS	8.58 ± 0.28 <sup>a</sup>	100.8 ± 2.1 <sup>f</sup>	16.01 ± 1.10 <sup>c</sup>	0.105 ± 0.010 <sup>a</sup>	0.21 ± 0.03 <sup>b</sup>	0.12 ± 0.01 <sup>d</sup>	5.12 ± 0.25 <sup>d</sup>	5.27 ± 0.16 <sup>d</sup>	18.75 ± 0.90 <sup>d</sup>	2.28 ± 0.11 <sup>e</sup>
BS	8.64 ± 0.33 <sup>a</sup>	141.5 ± 3.3 <sup>d</sup>	23.17 ± 1.28 <sup>b</sup>	0.066 ± 0.005 <sup>bc</sup>	0.11 ± 0.01 <sup>c</sup>	0.18 ± 0.01 <sup>d</sup>	3.31 ± 0.16 <sup>e</sup>	1.46 ± 0.27 <sup>e</sup>	32.30 ± 1.30 <sup>a</sup>	3.72 ± 0.18 <sup>d</sup>
ZS	8.68 ± 0.43 <sup>a</sup>	197.7 ± 4.9 <sup>a</sup>	29.95 ± 1.40 <sup>a</sup>	0.031 ± 0.002 <sup>d</sup>	0.16 ± 0.01 <sup>b</sup>	0.63 ± 0.03 <sup>b</sup>	11.6 ± 0.58 <sup>b</sup>	6.10 ± 0.31 <sup>cd</sup>	26.60 ± 1.33 <sup>bc</sup>	2.10 ± 0.11 <sup>e</sup>
FS	8.56 ± 0.41 <sup>a</sup>	119.2 ± 2.9 <sup>e</sup>	18.46 ± 1.21 <sup>c</sup>	0.038 ± 0.002 <sup>d</sup>	0.20 ± 0.02 <sup>b</sup>	0.60 ± 0.03 <sup>b</sup>	0.32 ± 0.15 <sup>f</sup>	0.84 ± 0.05 <sup>e</sup>	26.52 ± 1.21 <sup>bc</sup>	8.12 ± 0.51 <sup>a</sup>

**H**, water sample from El-Hamra Lake; **Z**, water sample from Zugm Lake; **B**, water sample from Beida Lake; **F\***, no water sample could be collected from El-Fazda Lake during the sampling campaign; **HS**, sediment sample from El-Hamra Lake; **BS**, sediment sample from Beida Lake; **ZS**, sediment sample from Zugm Lake; **FS**, sediment sample from El-Fazda Lake; **N.D.**, not determined. Different letters in the same column indicate significant statistical difference (*p*<0.05); e.g., “b” and “c” are statistically different from each other but not from “bc”.

### 3.2. PCR-DGGE Analysis

The archaeal phylogenetic diversity was studied by PCR-DGGE of 16S rRNA gene fragments (Figure 2). As can be appraised in Figure 3, the archaeal DGGE profiles were complex and presented an average of 134 bands, often comprising of 17 to 19 more intensely stained bands. The number of DGGE bands, considered indicative of the total species richness, did not vary considerably between all of the analyzed samples, and this result matched with the values calculated for different diversity indexes (Table 3) [59,60].



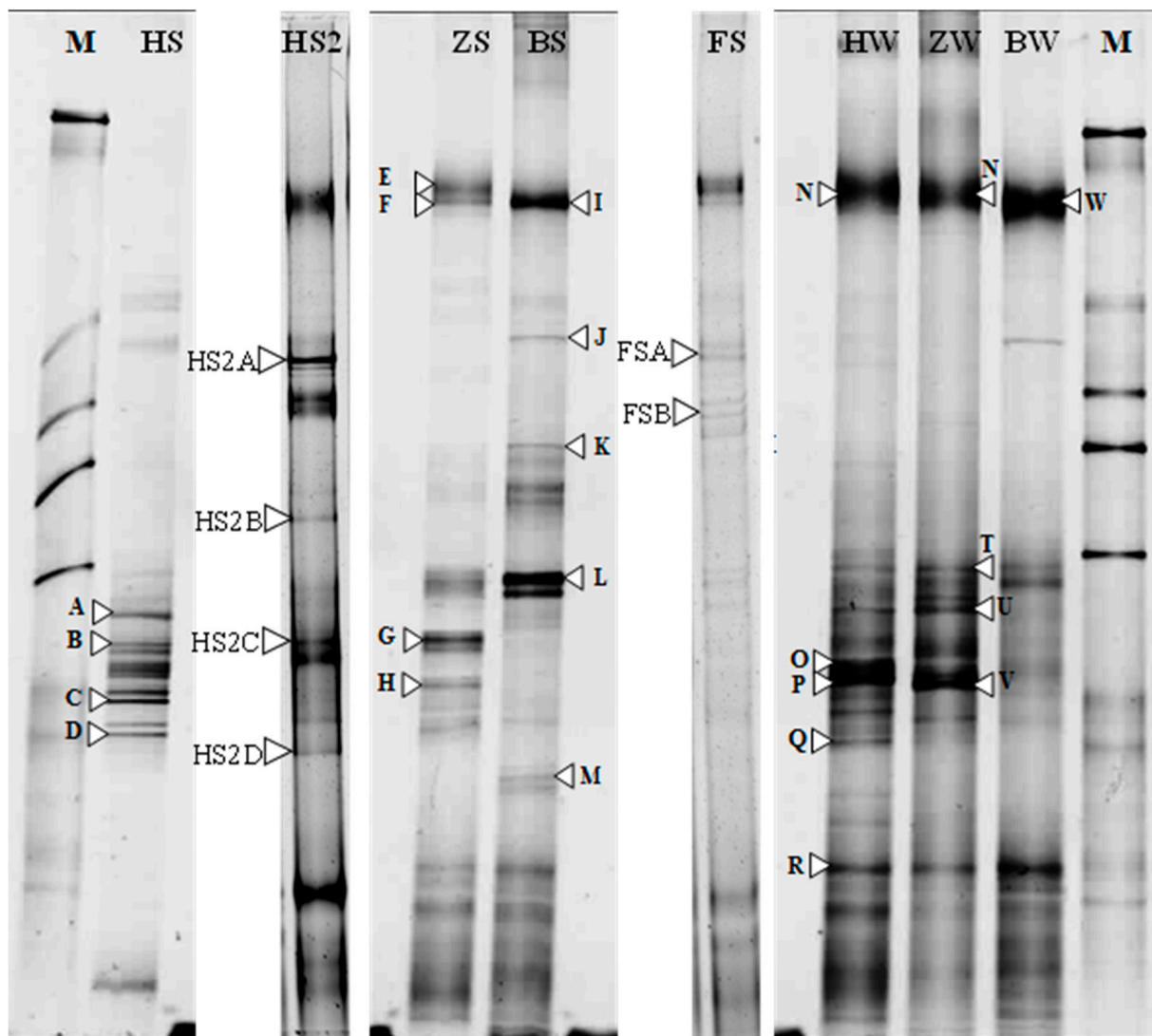
**Figure 2.** 16S rRNA PCR-amplification products of DNA extracted from water and sediment/salt crystal samples from soda lakes in Wadi El-Natron. Lane –ve: without DNA (control); Lane M: 1 kb DNA ladder; Lanes HS1 and HS2: sediment and salt crystals from El-Hamra Lake, respectively; Lane ZS: sediment from Zugm Lake; Lane BS: salt crystals from Beida Lake; Lane FS: sediment sample from El-Fazda Lake; Lanes HW, ZW and BW: water samples from El-Hamra, Zugm, and Beida lakes, respectively.

In general, our results agreed with previous studies regarding the microbial diversity found in other alkaline lakes. For example, in a study conducted by [61], the authors reported the presence of 10 to 20 bands in the DGGE profiles obtained for water samples from the Faro saline lake, a meromictic lagoon located to the northeast of Sicily (Messina, Italy). In another related work, [62] analyzed the prokaryotic diversity in water samples collected from the Aran-Bidgol lake, a thalassohaline lake in Iran. In such work, the DGGE patterns of the archaeal diversity showed ~15 intensively stained bands. Most of the archaeal sequences analyzed were related to *Haloquadratum walsbyi* (40%), followed by *Halorubrum* sp. (25%), *Halonotius* sp. (12.5%), *Halorhabdus* sp. (12.5%), and *Haladaptatus* sp. (10%).

**Table 3.** Diversity and richness indices for archaeal clone libraries.

Data Type	Sediment Samples				Water Samples			
	El-Hamra	Zugm	Beida	El-Fazda	El-Hamra	Zugm	Beida	El-Fazda
S	17	16	20	12	18	16	14	N.D.
N	706	600	1270	608	1286	1235	977	N.D.
Shannon (S)	2.65	2.70	2.75	2.24	2.67	2.65	2.48	N.D.
Margalef’s index	2.43	2.34	2.65	1.46	2.37	2.10	1.80	N.D.
Evenness index (e)	0.156	0.169	0.130	0.094	0.153	0.165	0.170	N.D.

S, total number of species (bands). N, total number of individuals (relative band intensity) N.D., not determined.



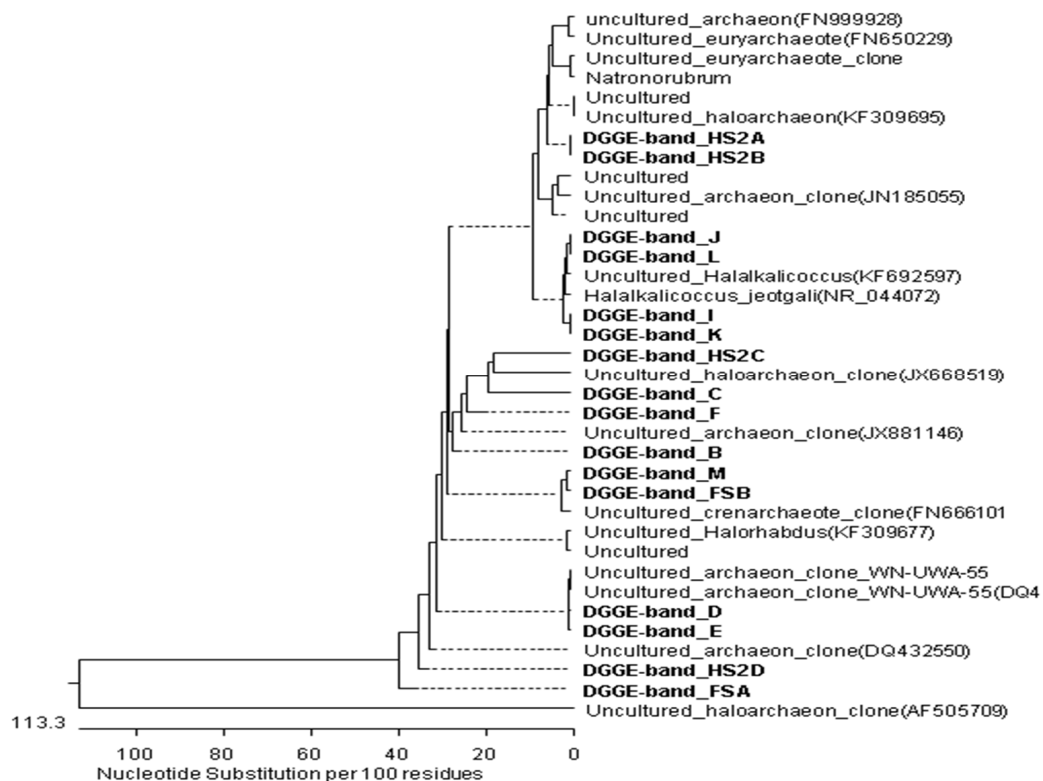
**Figure 3.** Archaeal 16S rRNA gene targeted PCR-DGGE analysis of sediment/salt crystal and water samples from soda lakes of Wadi El-Natron. Lane M: molecular weight marker (Kbp); Lane HS: sediment sample of Hamra Lake; Lane HS2: salt crystals of Hamra Lake; Lane ZS: salt crystals of Zugm Lake; Lane BS: salt crystals of El-Beida Lake; Lane FS: sediment of Fazda Lake; Lane HW: water sample of Hamra Lake; Lane ZW: water of Zugm Lake; and Lane BW: water of El-Beida Lake.

On the other hand, several studies have demonstrated that the microbial community in many hypersaline environments is dominated by halophilic archaea [6,7,9,10,12,15,26,33–36,47,56,61,62]. As can be seen in Table 4, our results show that 9 out of 15 phylotypes (bands B, C, K, Q, R, V, HS2A, HS2D, and FSA) were vaguely linked to uncultured clones ( $\leq 95\%$ ). In addition, two other bands (C and N) were associated with uncultured clones of *Halorubdus* and *Halorubrum* with similarities of 93% and 97%, respectively. Five other bands (B, J, K, L, and HS2C) were associated with *Halogranum*, *Halalkalicoccus*, and *Natronorubrum*, with similarities of 94%, 95%, and 98%, respectively (Table 4). In addition, the phylogenetic tree depicted in Figure 4 shows that the archaeal community is small, in agreement with other studies assessing the diversity of halophilic archaea in related saline environments [61–67]. However, it is noteworthy that most clones found in our study exhibited low sequence similarity with formerly recognized species (Table 4), suggesting the presence of new archaeal phylotypes in the soda lakes of Wadi El-Natron.

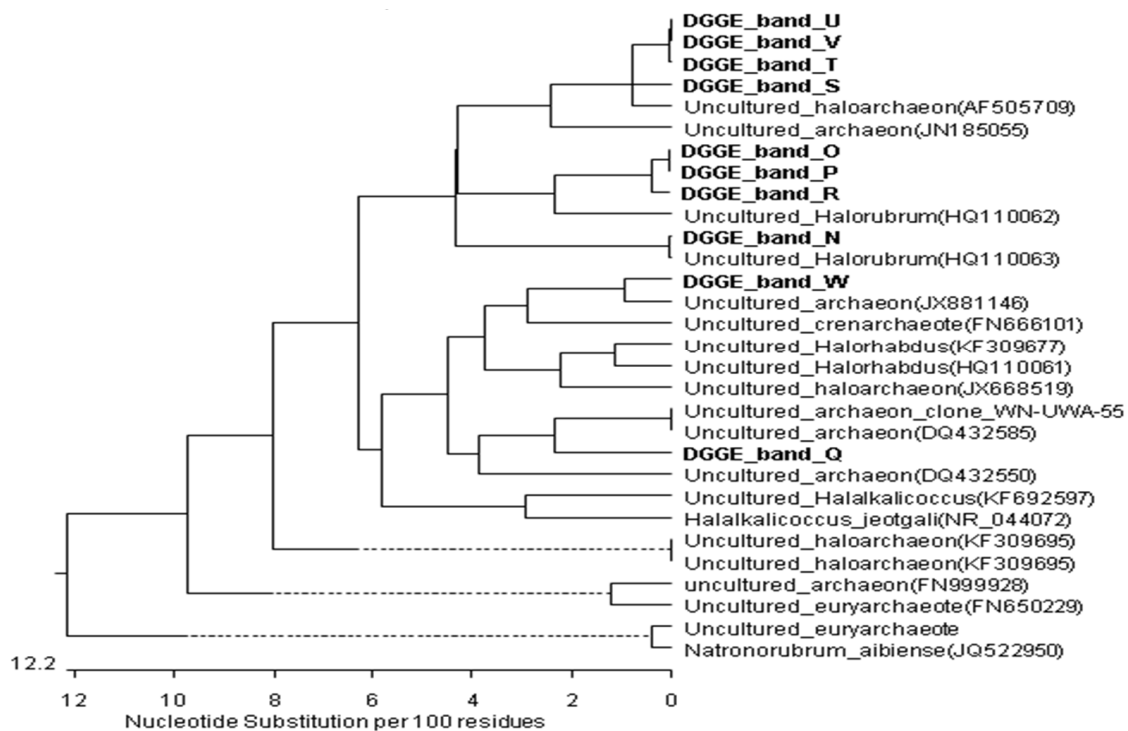


**Table 4.** Blast results of archaeal 16S rRNA sequences obtained from DGGE analysis.

Band	Close Relative in Database (Accession Number)	Taxonomic Description	Similarity (%)
B	<i>Halogramum</i> sp. SS5-1 (JN196479.1)		94
C	Uncultured <i>Halorhabdus</i> sp. clone M3-B02 (KF452246)		93
D	Uncultured archaeon clone WN-UWA-55 (DQ432585.1)		96
E	Uncultured archaeon clone WN-UWA-55 (DQ432585.1)		97
F	Uncultured archaeon clone CBA3919.b1 (JX881146.1)		97
I	Uncultured archaeon clone WN-FWA-110 (DQ432514)	<i>Euryarchaeota</i>	99
J	<i>Halalkalicoccus tibetensis</i> : JCM 11,890 (AB663349)		98
K	<i>Halalkalicoccus jeotgali</i> B3 (NR_102920.1)		95
L	<i>Halalkalicoccus jeotgali</i> strain: JCM 14,584 (AB477223)		98
M	Uncultured haloarchaeon clone TX4CA_31 (EF690586.1)		97
N	Uncultured <i>Halorubrum</i> sp. isolate DGGE gel band JG06 (HQ110063)		97
O	Archaeon DSFBPS_UR1C (KC465572)	Unclassified	97
P	Archaeon DSFBPG_5R3A (KC465564)	Archaea	99
Q	<i>Halobacteriaceae</i> archaeon YC93 (JQ237117.1)		90
R	Uncultured euryarchaeote clone FR-M-R-S1-B11 (KC661808)		92
S	Uncultured haloarchaeon clone TX4CA_24 (EF690579)	<i>Euryarchaeota</i>	98
T	Uncultured haloarchaeon clone ZB-A56 (AF505709)		98
U	Uncultured archaeon clone ARC182 (JN185055)		97
V	Uncultured haloarchaeon clone TX4CA_24 (EF690579)		93
W	Uncultured crenarchaeote clone P1A2RS32 (FN666101)	<i>Crenarchaeota</i>	97
HS2A	Uncultured haloarchaeon clone HPA-18 (AY430113.1)		93
HS2B	Uncultured haloarchaeon isolate DGGE gel band ESSA-A1_12 (KF309695)		98
HS2C	<i>Natronorubrum aibiense</i> strain G23 (JQ522950)	<i>Euryarchaeota</i>	98
HS2D	Uncultured archaeon clone WN-USA-38 (DQ432550)		94
FSA	Uncultured archaeon clone WN-USA-38(DQ432550)		94
FSB	Uncultured archaeon clone P11_3-7C (KF814487)		98



**Figure 4.** Cont.



**Figure 4.** Phylogenetic tree showing the relationships of archaeal 16S rRNA gene sequences of excised DGGE bands to closely related ( $S \geq 90\%$ ) sequences from the GenBank database.

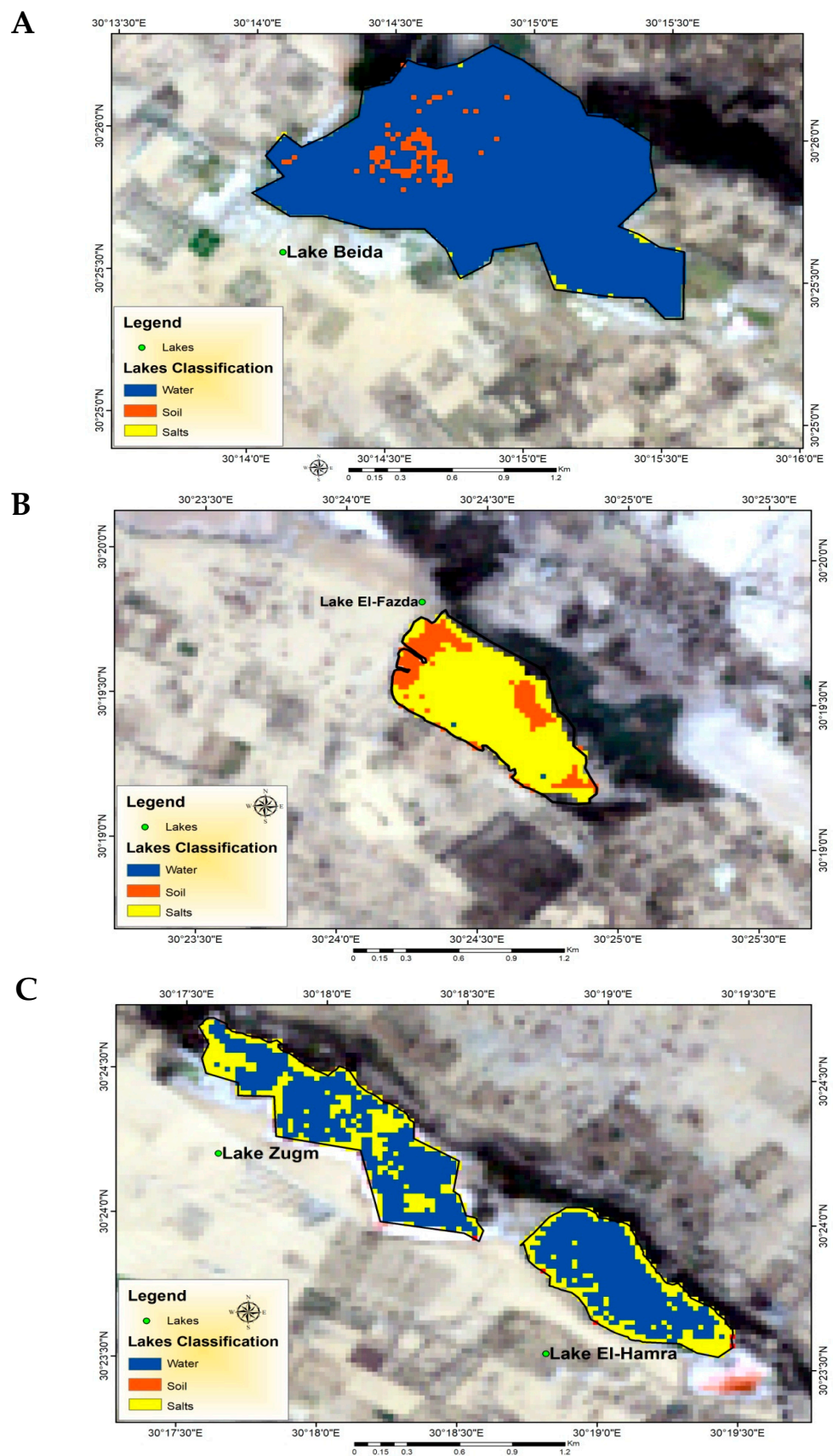
### 3.3. Spatial Distribution of Archaeal DNA by GIS and Remote Sensing

Remote sensing and GIS are highly accepted techniques for monitoring lake surfaces and detection of changes [5,68–70]. In this survey, the obtained map after classification discriminated the four analyzed lakes into three different areas, namely water (deep and shallow zones), salts and soil. This classification depends on the reflectance of each of these features according to a suitable threshold (Figure 5).

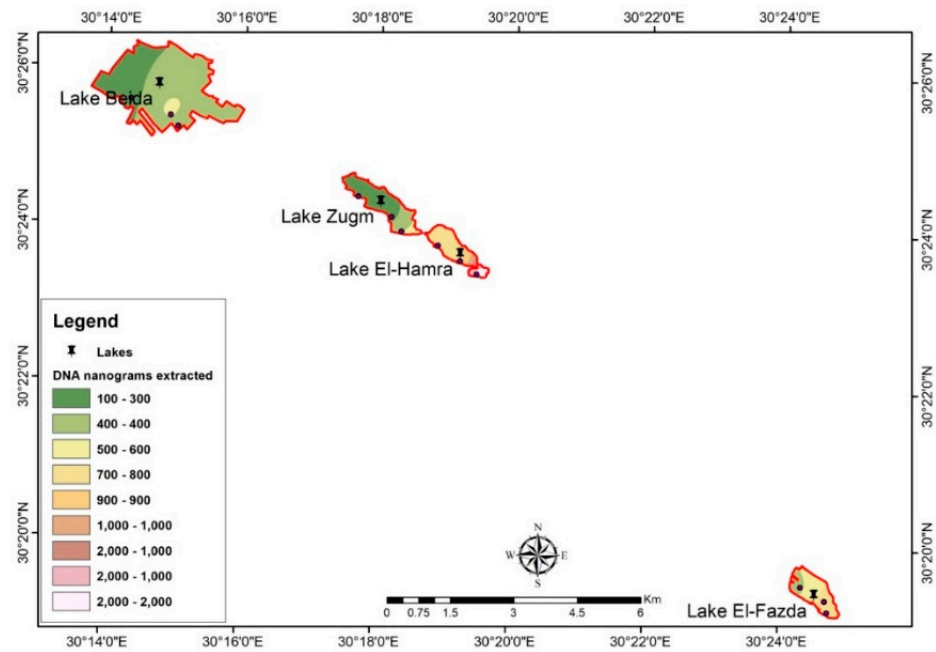
It should be noted that the water content is different in El-Fazda Lake according to the season since it dries up in summer and re-fills in winter, mostly affecting the salt content of the shallow zones. Still, the classification map obtained for the Wadi El-Natron lakes agreed with previous studies using similar methods wherein the analyzed areas were associated with marshlands and sabkhas [5,68,69,71].

On the other hand, Figures 6–8 illustrate the microbial DNA distribution map obtained with GIS technology according to the type of sample analyzed (i.e., sediment/salt crystals or water samples) from the four studied soda lakes. As can be appraised in Figure 6, the total content of DNA (expressed in nanograms) was the lowest for both Beida and Zugm lakes, with values ranging from 199.3 to 448.2 ng.

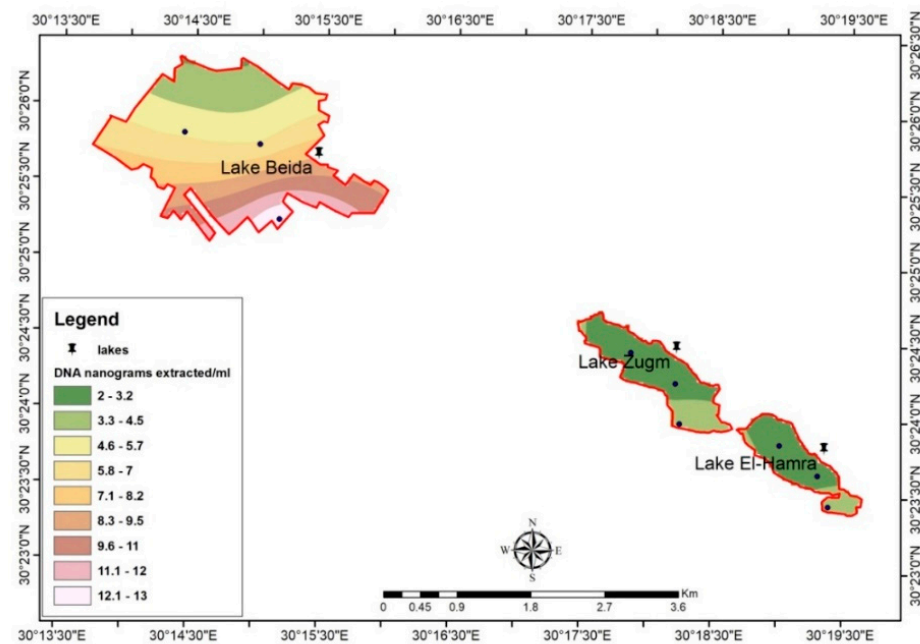
The GIS spatial distribution map of DNA (ng/mL) extracted from water samples analyzed from the soda lakes in Wadi El-Natron showed that Zugm and El-Hamra lakes presented the minimum values, ranging from 2.0 to 4.5 ng/mL (Figure 7). On the other hand, microbial DNA content (ng/mL) of water samples from Beida Lake decreased from the southern (maximal values ~13.0 ng/mL) to northern areas (Figure 7). It should be noted that there were no data for El-Fazda lake because it was dry during the sampling campaign and only contained sediment. Finally, microbial DNA extracted from sediments/salts crystal expressed as ng/g showed a great dispersion among lakes (Figure 8). The minimum microbial DNA values were obtained from Beida Lake, and the highest values corresponded to samples analyzed from El-Hamra Lake, followed by El-Fazda Lake.



**Figure 5.** Classification map of (A) Beida Lake, (B) El-Fazda Lake, and (C) El-Hamra and Zugm Lakes showing different environmental zones (water = blue, soil = orange, and salts = yellow).



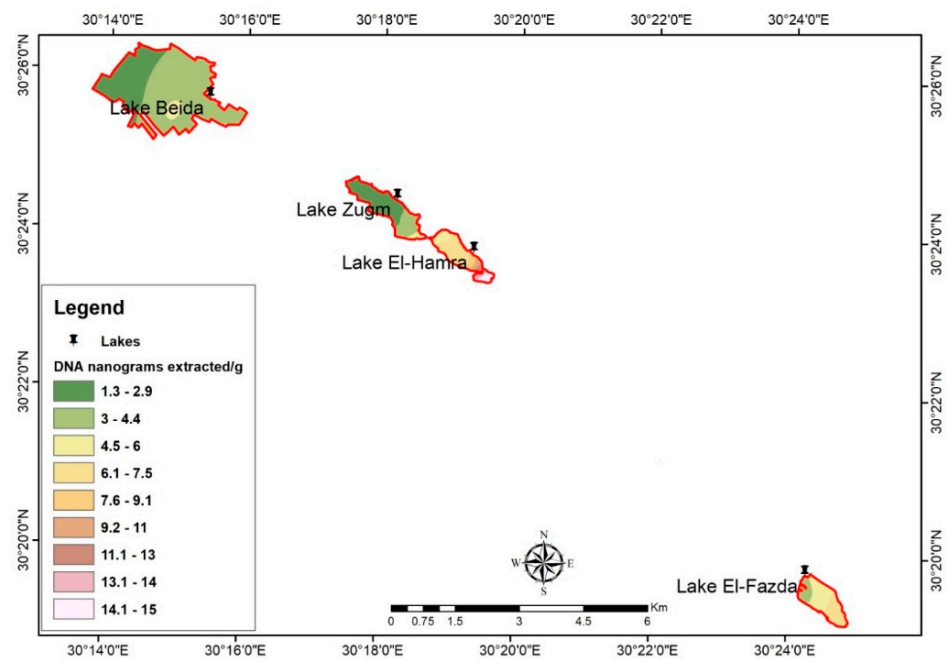
**Figure 6.** Spatial distribution by GIS of total DNA (ng) extracted from soda lakes of Wadi El-Natron.



**Figure 7.** Spatial distribution by GIS of DNA (ng/mL) extracted from water samples of Wadi El-Natron soda lakes. Note that the El-Fazda lake was dry during the sampling campaign and only contained sediment.

### 3.4. Spatial Distribution of Archaeal 16S rRNA Gene by GIS

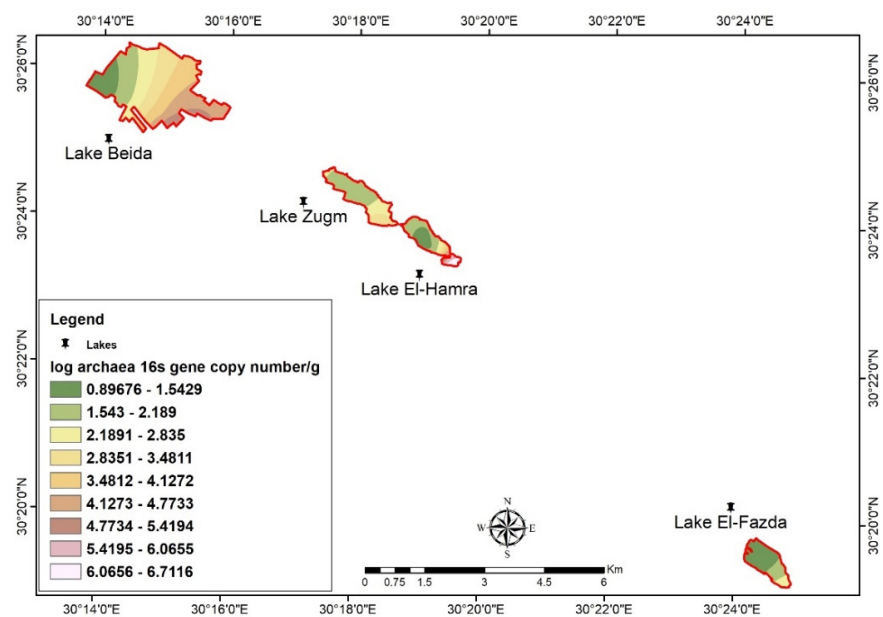
Figure 9 shows the distribution and abundance of total *Archaea* in sediment (Figure 9A) and water (Figure 9B) samples from Wadi El-Natron soda lakes determined by *qPCR* and reported as 16S rRNA gene copy number per gram of wet sediment or mL of brine, respectively. The abundance of *Archaea* was  $6.5 \times 10^8$  copies/g in sediment samples from El-Hamra Lake, followed by Beida Lake ( $5.0 \times 10^7$  copies/g), while in sediment samples from Zugm and El-Fazda lakes, the abundance of archaeal DNA was much lower ( $2.2 \times 10^8$  and  $2.3 \times 10^8$  copies/g, respectively).



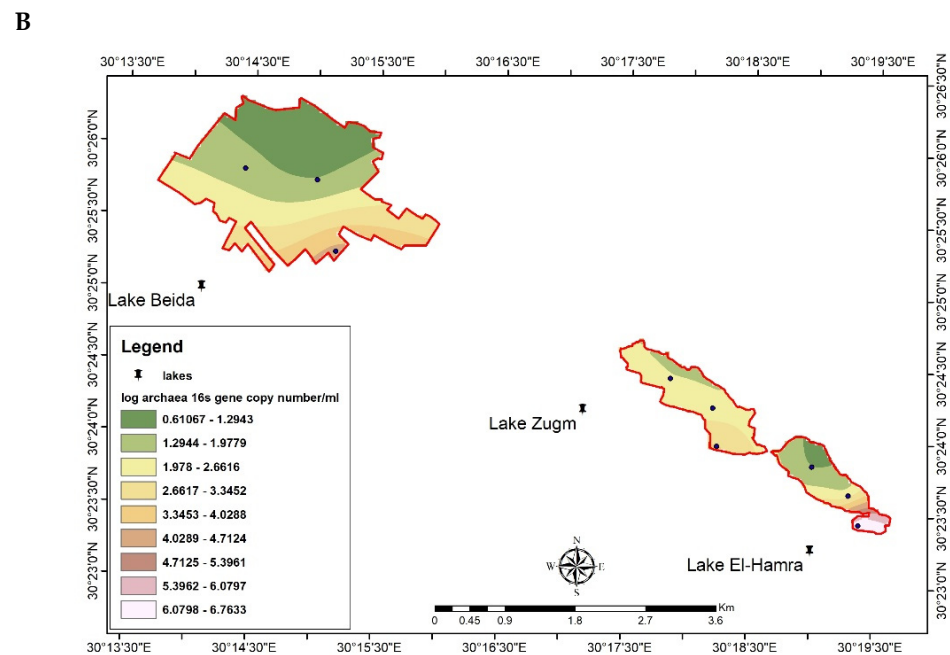
**Figure 8.** Spatial distribution by GIS of DNA (ng/g) extracted from sediment/salt crystal samples of Wadi El-Natron soda lakes.

On the other hand, 16S rRNA gene copy number per ml of brine was  $6.7 \times 10^8$  copies/g in El-Hamra Lake, followed by Zugm Lake ( $4.7 \times 10^8$  copies/g) and El-Beida Lake ( $4.2 \times 10^8$  copies/g). Notably, we observed a strong positive correlation (Pearson's  $r = 0.985$ ) between the content of 16S rRNA gene and the  $K^+$  concentration in all of the analyzed samples. This result may be explained by the fact that halophilic archaea accumulate molar quantities of KCl (as an osmoprotectant) due to the occurrence of acidic proteomes in their cytoplasm that only function at high salinity [21,72,73]. In addition, our results also showed clear differences between the numbers of 16S gene copies in water, sediments, and salts of the studied lakes.

**A**



**Figure 9.** Cont.



**Figure 9.** DNA copy number distribution of the archaeal 16S rRNA gene (A) per gram of sediment and (B) per mL of water from soda lakes of Wadi El-Natrun.

#### 4. Conclusions

The distribution of any organism in the environment is restricted to the physico-chemical characteristics of the sampling site. Soda lakes are rare and extreme ecosystems with great potential for bioprospecting aimed at discovering novel enzyme or genes for new biotechnological applications. This report provides a first representation of the archaeal community structure and spatial distribution in four soda lakes located in the Wadi El-Natrun valley (northern Egypt) using 16S rRNA PCR-DGGE fingerprinting and combining traditional GIS mapping technology with remote sensing. Using these approaches, we increased the scope and power of the analysis, making possible the mapping of unexplored areas wherein the diversity of alkaliphilic *Haloarchaea* are typically low. Our results revealed that the microbial community inhabiting these alkaline hypersaline environments appears to be rich in new types of *Archaea*. Therefore, the data presented here could serve as a promising starting point for future culture-dependent studies aimed at isolating and characterizing new archaeal species in order to reveal their ecological roles.

**Author Contributions:** Conceptualization S.S. and N.H.; methodology, N.E., A.H.M. and N.H.; formal analysis, S.S., N.H. and L.M.P.; visualization, E.M.M., F.A.S., S.M.A., M.S., S.S.A., I.H., A.S., L.M.P. and D.G.A.; writing—original draft preparation, N.E., A.H.M. and N.H.; writing—review and editing, E.M.M., F.A.S., S.M.A., A.S., D.G.A., M.S., S.S.A., I.H., S.S., A.E. and L.M.P.; supervision, S.S., E.M.M., F.A.S., S.M.A., A.S., M.S., S.S.A., I.H. and D.G.A.; resources and funding, E.M.M., F.A.S., M.S., S.S.A., I.H., S.M.A., A.S. and D.G.A.; project administration, S.S. All authors have read and agreed to the published version of the manuscript.

**Funding:** Princess Nourah bint Abdulrahman University Researchers supporting Project number (PNURSP2022R318), Princess Nourah bint Abdulrahman University; Riyadh; Saudi Arabia.

**Institutional Review Board Statement:** Not applicable.

**Informed Consent Statement:** Not applicable.

**Data Availability Statement:** Not applicable.

**Acknowledgments:** The authors extend their appreciation to the Princess Nourah bint Abdulrahman University Researchers Supporting Project number (PNURSP2022R318), Princess Nourah bint Abdulrahman University, Riyadh, Saudi Arabia, and many thanks to Roberta Gorra, Department of

Agricultural, Forest and Food Sciences, University of Torino, for her valuable supervision during DGGE analysis.

**Conflicts of Interest:** The funders had no role in the design of the study; in the collection, analyses, or interpretation of data; in the writing of the manuscript, or in the decision to publish the results.

## References

- Sayed, M.F.; Abdo, M.H. Assessment of environmental impact on, Wadi El-Natron depression lakes water, Egypt. *World J. Fish Mar. Sci.* **2009**, *1*, 129–136. Available online: [https://www.idosi.org/wjfm/wjfm1\(2\)09/9.pdf](https://www.idosi.org/wjfm/wjfm1(2)09/9.pdf) (accessed on 20 February 2022).
- Taher, A. Inland saline lakes of Wadi El Natrun depression, Egypt. *Int. J. Salt Lake Res.* **1999**, *8*, 149–169. [[CrossRef](#)]
- Boros, E.; Kolpakova, M. A review of the defining chemical properties of soda lakes and pans: An assessment on a large geographic scale of Eurasian inland saline surface waters. *PLoS ONE* **2018**, *13*, e0202205. [[CrossRef](#)] [[PubMed](#)]
- El-Malky, M.; Shalaby, A.; Khalifa, A.; Gabreel, M. Impact of agricultural expansion and urbanization on groundwater quality using spatial analysis of GIS and remote sensing techniques at Wadi El-Natron area, Egypt. *J. Environ. Sci.* **2017**, *40*, 23–50.
- Masoud, A.; Atwia, A.M.G. Spatio-temporal characterization of the Pliocene aquifer conditions in Wadi El-Natron area, Egypt. *Environ. Earth Sci.* **2011**, *62*, 1361–1374. [[CrossRef](#)]
- Sorokin, D.Y.; Kuenen, J.G. Alkaliphilic chemolithotrophs from sodas lakes. *FEMS Microbiol. Ecol.* **2005**, *52*, 287–295. [[CrossRef](#)]
- Foti, M.J.; Sorokin, D.Y.; Zacharova, E.E.; Pimenov, N.V.; Kuenen, J.G.; Muyzer, G. Bacterial diversity and activity along a salinity gradient in soda lakes of the Kulunda Steppe (Altai, Russia). *Extremophiles* **2008**, *12*, 133–145. [[CrossRef](#)]
- Sorokin, D.Y.; van Pelt, S.; Tourova, T.P.; Muyzer, G. Microbial isobutyronitrile utilization under haloalkaline conditions. *Appl. Environ. Microbiol.* **2007**, *73*, 5574–5579. [[CrossRef](#)]
- Rees, H.C.; Grant, W.D.; Jones, B.E.; Heaphy, S. Diversity of Kenyan soda lake alkaliphiles assessed by molecular methods. *Extremophiles* **2004**, *8*, 63–71. [[CrossRef](#)]
- Oremland, R.S.; Stolz, J.F.; Hollibaugh, J.T. The microbial arsenic cycle in Mono Lake, California. *FEMS Microbiol. Ecol.* **2004**, *48*, 15–27. [[CrossRef](#)]
- Oremland, R.S.; Kulp, T.R.; Blum, J.S.; Hoefft, S.E.; Baesman, S.; Miller, L.G.; Stolz, J.F. A microbial arsenic cycle in a salt-saturated, Extreme environment. *Science* **2005**, *308*, 1305–1308. [[CrossRef](#)] [[PubMed](#)]
- Mesbah, N.M.; Abou-El-Ela, S.H.; Wiegel, J. Novel and unexpected prokaryotic diversity in water and sediments of the alkaline, hypersaline lakes of the Wadi An Natrun, Egypt. *Microb. Ecol.* **2007**, *54*, 598–617. [[CrossRef](#)] [[PubMed](#)]
- Enache, M.; Itoh, T.; Fukusguna, T.; Usami, R.; Dumitru, L.; Kamekura, M. Phylogenetic relationships within the family *Halobacteriaceae* inferred from *rpoB'* gene and protein sequences. *Int. J. Syst. Evol. Microbiol.* **2007**, *57*, 2289–2295. [[CrossRef](#)] [[PubMed](#)]
- Oren, A. Taxonomy of the family *Halobacteriaceae*: A paradigm for changing concepts in prokaryote systematics. *Int. J. Syst. Evol. Microbiol.* **2012**, *62*, 263–271. [[CrossRef](#)]
- Sorokin, D.Y.; Messina, E.; Smedile, F.; Roman, P.; Damste, J.S.S.; Ciordia, S.; Mena, M.C.; Ferrer, M.; Golyshin, P.N.; Kublanov, I.V.; et al. Discovery of anaerobic lithoheterotrophic haloarchaea, ubiquitous in hypersaline habitats. *ISME J.* **2017**, *11*, 1245–1260. [[CrossRef](#)]
- Minegishi, H.; Enomoto, S.; Echigo, A.; Shimane, Y.; Kondo, Y.; Inoma, A.; Kamekura, M.; Takai, K.; Itoh, T.; Ohkuma, M.; et al. *Salinarchaeum chitinilyticum* sp. nov., a chitin-degrading haloarchaeon isolated from commercial salt. *Int. J. Syst. Evol. Microbiol.* **2017**, *67*, 2274–2278. [[CrossRef](#)]
- Zhou, Y.; Li, Y.; Lü, Z.Z.; Cui, H.L. *Halomarina rubra* sp. nov., isolated from a marine solar saltern. *Arch. Microbiol.* **2017**, *199*, 1431–1435. [[CrossRef](#)]
- Sorokin, D.Y.; Khijniak, T.V.; Elcheninov, A.G.; Toshchakov, S.V.; Kostrikina, N.A.; Bale, N.J.; Sinninghe Damsté, J.S.; Kublanov, I.V. *Halococcoides cellulovorans* gen. nov., sp. nov., an extremely halophilic cellulose-utilizing haloarchaeon from hypersaline lakes. *Int. J. Syst. Evol. Microbiol.* **2019**, *69*, 1327–1335. [[CrossRef](#)]
- Youssef, N.H.; Savage-Ashlock, K.N.; McCully, A.L.; Luedtke, B.; Shaw, E.I.; Hoff, W.D.; Elshahed, M.S. Trehalose/2-sulfotrehalose biosynthesis and glycine-betaine uptake are widely spread mechanisms for osmoadaptation in the *Halobacteriales*. *ISME J.* **2014**, *8*, 636–649. [[CrossRef](#)]
- Grant, W.D.; Gemmell, R.T.; McGenity, T.J. Halobacteria: The evidence for longevity. *Extremophiles* **1998**, *2*, 279–287. [[CrossRef](#)]
- Oren, A. Life at high salt concentrations, intracellular KCl concentrations, and acidic proteomes. *Front. Microbiol.* **2013**, *4*, 315. [[CrossRef](#)] [[PubMed](#)]
- Oren, A.; Pri-El, N.; Shapiro, O.; Siboni, N. Buoyancy studies in natural communities of square gas-vacuolate archaea in saltern crystallizer ponds. *Saline Syst.* **2006**, *2*, 4. [[CrossRef](#)] [[PubMed](#)]
- Soppa, J. From genomes to function: *Haloarchaea* as model organisms. *Microbiology* **2006**, *152*, 585–590. [[CrossRef](#)] [[PubMed](#)]
- Tsiamis, G.; Katsaveli, K.; Ntougias, S.; Kyripides, N.; Andersen, G.; Piceno, Y.; Bourtzis, K. Prokaryotic community profiles at different operational stages of a Greek solar saltern. *Res. Microbiol.* **2008**, *159*, 609–627. [[CrossRef](#)]
- Kharroub, K.; Quesada, T.; Ferrer, R.; Fuentes, S.; Aguilera, M.; Boulahrouf, A.; Ramos-Cormenzana, A.; Monteoliva-Sánchez, M. *Halorubrum ezzeoulense* sp. nov., a halophilic archaeon isolated from Ezzemoul sabkha, Algeria. *Int. J. Syst. Evol. Microbiol.* **2006**, *56*, 1583–1588. [[CrossRef](#)] [[PubMed](#)]

26. Luque, R.; González-Domenech, C.M.; Llamas, I.; Quesada, E.; Béjar, V. Diversity of culturable halophilic archaea isolated from Rambla Salada, Murcia (Spain). *Extremophiles* **2012**, *16*, 205–213. [[CrossRef](#)]
27. Sorokin, D.Y.; Berben, T.; Melton, E.D.; Overmars, L.; Vavourakis, C.D.; Muyzer, G. Microbial diversity and biogeochemical cycling in soda lakes. *Extremophiles* **2014**, *18*, 791–809. [[CrossRef](#)] [[PubMed](#)]
28. Williams, T.J.; Allen, M.A.; DeMaere, M.Z.; Kyrpides, N.C.; Tringe, S.G.; Woyke, T.; Cavicchioli, R. Microbial ecology of an antarctic hypersaline lake: Genomic assessment of ecophysiology among dominant haloarchaea. *ISME J.* **2014**, *8*, 1645–1658. [[CrossRef](#)] [[PubMed](#)]
29. Parte, A.C.; Sardà Carbasse, J.; Meier-Kolthoff, J.P.; Reimer, L.C.; Göker, M. List of prokaryotic names with standing in nomenclature (LPSN) moves to the DSMZ. *Int. J. Syst. Evol. Microbiol.* **2020**, *70*, 5607–5612. [[CrossRef](#)] [[PubMed](#)]
30. Ventosa, A.; Nieto, J.J. Biotechnological applications, and potentialities of halophilic microorganisms. *World J. Microbiol. Biotechnol.* **1995**, *11*, 85–94. [[CrossRef](#)]
31. Schiraldi, C.; Mariateresa, G.; Mario, D. Perspectives on biotechnological applications of archaea. *Archaea* **2002**, *1*, 75–86. [[CrossRef](#)]
32. Hamad, A.A.; Sharaf, M.; Hamza, M.A.; Selim, S.; Hetta, H.F.; El-Kazzaz, W. Investigation of the Bacterial Contamination and Antibiotic Susceptibility Profile of Bacteria Isolated from Bottled Drinking Water. *Microbiol. Spectr.* **2022**, *10*, e01516-21. [[CrossRef](#)] [[PubMed](#)]
33. Najjari, A.; Elshahed, M.S.; Cherif, A.; Youssef, N.H. Patterns and determinants of halophilic archaea (Class Halobacteria) diversity in Tunisian endorheic salt lakes and sebkhet systems. *Appl. Environ. Microbiol.* **2015**, *81*, 4432–4441. [[CrossRef](#)] [[PubMed](#)]
34. Baati, H.; Guermazi, S.; Amdouni, R.; Gharsallah, N.; Sghir, A.; Ammar, E. Prokaryotic diversity of a Tunisian multipond solar saltern. *Extremophiles* **2008**, *12*, 505–518. [[CrossRef](#)] [[PubMed](#)]
35. Youssef, N.H.; Ashlock-Savage, K.N.; Elshahed, M.S. Phylogenetic diversities and community structure of members of the extremely halophilic archaea (Order Halobacteriales) in multiple saline sediment habitats. *Appl. Environ. Microbiol.* **2012**, *78*, 1332–1344. [[CrossRef](#)] [[PubMed](#)]
36. Henriot, O.; Fourmentin, J.; Delincé, B.; Mahillon, J. Exploring the diversity of extremely halophilic archaea in food-grade salts. *Int. J. Food Microbiol.* **2014**, *191*, 36–44. [[CrossRef](#)] [[PubMed](#)]
37. Durán-Viseras, A.; Andrei, A.-S.; Ghai, R.; Sánchez-Porro, C.; Ventosa, A. New halonotius species provide genomics-based insights into cobalamin synthesis in *Haloarchaea*. *Front. Microbiol.* **2019**, *10*, 1928. [[CrossRef](#)]
38. Duarte, S.; Cássio, F.; Pascoal, C. Denaturing gradient gel electrophoresis (DGGE) in microbial ecology-insights from freshwaters. In *Gel Electrophoresis-Principles and Basics*; Magdeldin, S., Ed.; IntechOpen: Rijeka, Croatia, 2012; pp. 173–196. [[CrossRef](#)]
39. Tapia, E.; Donoso-Bravo, A.; Cabrol, L.; Alves, M.M.; Pereira, A.; Rapaport, A.; Ruiz-Filippi, G. A methodology for a functional interpretation of DGGE with the help of mathematical modelling. Application in bio-hydrogen production. *Water Sci. Technol.* **2014**, *69*, 511–517. [[CrossRef](#)]
40. Benítez-Cabello, A.; Bautista-Gallego, J.; Garrido-Fernández, A.; Rantsiou, K.; Cocolin, L.; Jiménez-Díaz, R.; Arroyo-López, F.N. RT-PCR–DGGE analysis to elucidate the dominant bacterial species of industrial Spanish-style green table olive fermentations. *Front. Microbiol.* **2016**, *7*, 1291. [[CrossRef](#)]
41. Sharaf, M.; Arif, M.; Khan, S.; Abdalla, M.; Shabana, S.; Chi, Z.; Liu, C. Co-delivery of hesperidin and clarithromycin in a nanostructured lipid carrier for the eradication of *Helicobacter pylori* in vitro. *Bioorganic Chem.* **2021**, *112*, 104896. [[CrossRef](#)]
42. Sörbo, B. Sulfate: Turbidometric and nephelometric methods. *Methods Enzymol.* **1987**, *143*, 3–6. [[CrossRef](#)] [[PubMed](#)]
43. Sharaf, M.; Sewid, A.H.; Hamouda, H.I.; Elharrif, M.G.; El-Demerdash, A.S.; Alharthi, A.; Hashim, N.; Hamad, A.A.; Selim, S.; Alkhalifah, D.H.M.; et al. Rhamnolipid-coated iron oxide nanoparticles as a novel multitarget candidate against major foodborne *E. coli* serotypes and methicillin-resistant *S. aureus*. *Microbiol. Spectrum* **2022**, e00250-22. [[CrossRef](#)]
44. Pérez, L.M.; Fittipaldi, M.; Adrados, B.; Morató, J.; Codony, F. Error estimation in environmental DNA targets quantification due to PCR efficiencies differences between real samples and standards. *Folia Microbiol.* **2013**, *58*, 657–662. [[CrossRef](#)] [[PubMed](#)]
45. Muyzer, G.; De, W.E.; Uitterlinden, A.G. Profiling of complex microbial populations by denaturing gradient gel electrophoresis analysis of polymerase chain reaction-amplified genes coding for 16S rRNA. *Appl. Environ. Microb.* **1993**, *59*, 695–700. [[CrossRef](#)] [[PubMed](#)]
46. Lucena-Padrós, H.; Jiménez, E.; Maldonado-Barragán, A.; Rodríguez, J.M.; Ruiz-Barba, J.L. PCR-DGGE assessment of the bacterial diversity in Spanish-style green table-olive fermentations. *Int. J. Food Microbiol.* **2015**, *205*, 47–53. [[CrossRef](#)] [[PubMed](#)]
47. Webster, G.; Parkes, R.J.; Cragg, B.A.; Newberry, C.J.; Weightman, A.J.; Fry, J.C. Prokaryotic community composition and biogeochemical processes in deep seafloor sediments from the Peru margin. *FEMS Microbiol. Ecol.* **2006**, *58*, 65–85. [[CrossRef](#)]
48. O’Sullivan, L.A.; Webster, G.; Fry, J.C.; Parkes, R.J.; Weightman, A.J. Modified linker-PCR primers facilitate complete sequencing of DGGE DNA fragments. *J. Microbiol. Methods* **2008**, *75*, 579–581. [[CrossRef](#)]
49. Altschul, S.F.; Madden, T.L.; Schaffer, A.A.; Zhang, J.; Zhang, Z.; Miller, W.; Lipman, D.J. Gapped BLAST and PSIBLAST: A new generation of protein database search programs. *Nucleic Acids Res.* **1997**, *25*, 3389–3402. [[CrossRef](#)]
50. Lane, D.J. 16S/23S rRNA Sequencing. In *Nucleic Acid Techniques in Bacterial Systematics*; Stackebrandt, E., Goodfellow, M., Eds.; John Wiley and Sons: New York, NY, USA, 1991; pp. 115–175.
51. Nicol, G.W.; Glover, L.A.; Prosser, J.I. Molecular analysis of methanogenic archaeal communities in managed and natural upland pasture soils. *Global Change Biol.* **2003**, *9*, 1451–1457. [[CrossRef](#)]



52. Øvreås, L.; Forney, L.; Daae, F.L.; Torsvik, V. Distribution of bacterioplankton in meromictic lake Saalen-vannet, as determined by denaturing gradient gel electrophoresis of PCR-amplified gene fragments coding for 16S rRNA. *Appl. Environ. Microbiol.* **1997**, *63*, 3367–3373. [[CrossRef](#)] [[PubMed](#)]
53. Sims, D.A.; Gamon, J.A. Estimation of vegetation water content and photosynthetic tissue area from spectral reflectance: A comparison of indices based on liquid water and chlorophyll absorption features. *Remote Sens. Environ.* **2003**, *84*, 526–537. [[CrossRef](#)]
54. Salem, S.M.; El Gammal, E.-S.A. Salt minerals at Wadi El Natrun saline lakes, Egypt. New implications from remote sensing data. *Eur. Chem. Bull.* **2018**, *7*, 72–80. [[CrossRef](#)]
55. DasSarma, S.; DasSarma, P. Halophiles and their enzymes: Negativity put to good use. *Curr. Opin. Microbiol.* **2015**, *25*, 120–126. [[CrossRef](#)] [[PubMed](#)]
56. Jabborova, D.; Annapurna, K.; Paul, S.; Kumar, S.; Saad, H.A.; Desouky, S.; Ibrahim, M.F.M.; Elkelish, A. Beneficial Features of Biochar and Arbuscular Mycorrhiza for Improving Spinach Plant Growth, Root Morphological Traits, Physiological Properties, and Soil Enzymatic Activities. *JoF* **2021**, *7*, 571. [[CrossRef](#)]
57. Sharaf, M.; Hamouda, H.; Shabana, S.; Khan, S.; Arif, M.; Rozan, H.E.; Abdallae, M.; Chia, Z.; Liu, C. Design of lipid-based nanocarrier for drug delivery has a double therapy for six common pathogens eradication. *Colloids Surfaces A: Physicochem. Eng. Aspects* **2021**, *625*, 126662. [[CrossRef](#)]
58. Grant, W.D. Alkaline environments. In *Encyclopaedia of Microbiology*, 1st ed.; Lederberg, J., Ed.; Academic Publishers: London, UK, 1992; pp. 73–80.
59. Shannon, C.E.; Wiener, W. *The Mathematical Theory of Communication*; University of Illinois Press: Urbana, IL, USA, 1949; p. 177.
60. Margalef, R. Temporal succession and spatial heterogeneity in phytoplankton. In *Perspectives in Marine Biology*; Buzzati-Traverso, A.A., Ed.; University of California Press: Berkeley, CA, USA, 1958; pp. 323–347.
61. Gugliandolo, C.; Lentini, V.; Maugeri, T. Distribution, and diversity of bacteria in a saline meromictic lake as determined by PCR-DGGE of 16S rRNA gene fragments. *Curr. Microbiol.* **2011**, *62*, 159–166. [[CrossRef](#)] [[PubMed](#)]
62. Makhdoumi-Kakhki, A.; Amoozegar, M.A.; Kazemi, B.; Pašić, L.; Ventosa, A. Prokaryotic diversity in Aran-Bidgol salt lake, the largest hypersaline playa in Iran. *Microbes Environ.* **2012**, *27*, 87–93. [[CrossRef](#)]
63. Cytryn, E.; Minz, D.; Oremland, R.S.; Cohen, Y. Distribution and diversity of archaea corresponding to the limnological cycle of a hypersaline stratified lake (Solar Lake, Sinai, Egypt). *Appl. Environ. Microbiol.* **2000**, *66*, 3269–3276. [[CrossRef](#)] [[PubMed](#)]
64. Sørensen, K.B.; Canfield, D.E.; Teske, A.P.; Oren, A. Community composition of a hypersaline endoevaporitic microbial mat. *Appl. Environ. Microbiol.* **2005**, *71*, 7352–7365. [[CrossRef](#)] [[PubMed](#)]
65. Ben Abdallah, M.; Karray, F.; Kallel, N.; Armougom, F.; Mhiri, N.; Quéméneur, M.; Cayol, J.-L.; Erauso, G.; Sayadi, S. Abundance and diversity of prokaryotes in ephemeral hypersaline lake Chott El Jerid using Illumina Miseq sequencing, DGGE and qPCR assays. *Extremophiles* **2018**, *22*, 811–823. [[CrossRef](#)]
66. Najjari, A.; Stathopoulou, P.; Elmnasri, K.; Hasnaoui, F.; Zidi, I.; Sghaier, H.; Ouzari, H.I.; Cherif, A.; Tsiamis, G. Assessment of 16S rRNA gene-based phylogenetic diversity of archaeal communities in halite-crystal salts processed from natural Saharan saline systems of Southern Tunisia. *Biology* **2021**, *10*, 397. [[CrossRef](#)]
67. Ochsenreiter, T.; Pfeifer, F.; Schleper, C. Diversity of *Archaea* in hypersaline environments characterized by molecular-phylogenetic and cultivation studies. *Extremophiles* **2002**, *6*, 267–274. [[CrossRef](#)]
68. Mohammed, A.B.; Mohamed, A.; El-Naggar, N.E.-A.; Mahrous, H.; Nasr, G.M.; Abdella, A.; Ahmed, R.H.; Irmak, S.; Elsayed, M.S.; Selim, S. Antioxidant and antibacterial activities of silver nanoparticles biosynthesized by *Moringa Oleifera* through response surface methodology. *J. Nanomater.* **2022**, *2022*, 9984308. [[CrossRef](#)]
69. Wei, L.; Zhang, Y.; Huang, C.; Wang, Z.; Huang, Q.; Yin, F.; Guo, Y.; Cao, L. Inland lakes mapping for monitoring water quality using a detail/smoothing-balanced conditional random field based on Landsat-8/levels data. *Sensors* **2020**, *20*, 1345. [[CrossRef](#)] [[PubMed](#)]
70. Hamed, A.F.; Salem, B.B.; El-Fatah, H.M.A. Floristic survey of blue-green algae/cyanobacteria in saline-alkaline lakes of Wadi El-Natrun (Egypt) by remote sensing application. *Res. J. Appl. Sci.* **2007**, *3*, 495–506. Available online: <http://www.aensiweb.com/old/jasr/jasr/2007/495-506.pdf> (accessed on 20 February 2022).
71. Arif, M.; Sharaf, M.; Samreen; Dong, Q.; Wang, L.; Chi, Z.; Liu, C.-G. Bacteria-targeting chitosan/carbon dots nanocomposite with membrane disruptive properties improve eradication rate of *Helicobacter pylori*. *J. Biomater. Sci. Polym. Ed.* **2021**, *32*, 2423–2447. [[CrossRef](#)] [[PubMed](#)]
72. Deole, R.; Challacombe, J.; Raiford, D.W.; Hoff, W.D. An extremely halophilic proteobacterium combines a highly acidic proteome with a low cytoplasmic potassium content. *J. Biol. Chem.* **2013**, *288*, 581–588. [[CrossRef](#)] [[PubMed](#)]
73. Selim, S.; Faried, O.A.; Almuhayawi, M.S.; Saleh, F.M.; Sharaf, M.; El Nahhas, N.; Warrad, M. Incidence of vancomycin-resistant *Staphylococcus aureus* strains among patients with urinary tract infections. *Antibiotics* **2022**, *11*, 408. [[CrossRef](#)]